Quantum Electronics **51** (6) 518–524 (2021) ©2021 Kvantovaya Elektronika and IOP Publishing Limited

 https://doi.org/10.1070/QEL17557

Influence of saturable absorber parameters on the operation regimes of a dumbbell-shaped thulium fibre laser

A.D. Zverev, V.A. Kamynin, A.I. Trikshev, E.Yu. Kovtun, N.R. Arutyunyan, A.A. Mastin, P.A. Ryabochkina, E.D. Obraztsova, V.B. Tsvetkov

Abstract. **The influence of saturable absorber parameters on the operation regimes of a dumbbell-shaped thulium fibre laser is studied. As saturable absorbers, polymer films with nanotubes characterised by different transmission coefficients in the saturated and unsaturated states are used. The operation of lasers with absorbers of different configurations used to obtain stable *Q*-switching and mode-locking regimes in the spectral range 1930–1960 nm is demonstrated. The average output power in the single-pulse mode-locking regime is 3.5 mW at a pulse repetition rate of 8.4 MHz and a pulse duration of 1.08 ps.**

Keywords: *thulium, fibre laser, passive mode locking, single-walled carbon nanotubes.*

1. Introduction

Fibre lasers emitting ultrashort pulses in the two-micron wavelength region have numerous applications. They are widely used in medicine, industry [1], and science [2, 3]. Ultrashort pulses of fibre lasers can be obtained in the passive mode-locking regime by using various nonlinear effects, namely, nonlinear polarisation plane rotation [4] and nonlinear optical loop mirror [5], or by introducing a saturable absorber into the laser cavity. As the latter, one can use SESAM semiconductor mirrors [6], films based on carbon nanotubes [7] of graphene [8], and topological insulators [9, 10].

Fibre lasers operating in the wavelength range 1.85–2.15 μm are based on optical fibres doped with thulium, holmium, or thulium–holmium complexes. A broad luminescence spectrum of thulium waveguides makes it possible to obtain pico- and femtosecond pulses. In particular, a thulium fibre laser with a nonlinear amplifying loop mirror and a semiconductor saturable absorber mirror or single-walled carbon nanotubes (SWCNTs) emitted pulses with durations of 230 and 450 fs, respectively [11]. A thulium laser with a ring-cavity [12] emitted 235-fs pulses due to nonlinear polarisation plane rotation. To achieve passive mode locking with 750-fs pulses in a thulium laser with a dumbbell-shaped cavity, Kieu and Wise [13] used carbon nanotubes as a saturable absorber.

The modulation depth and the optical losses introduced into the cavity by saturable absorbers used to achieve passive mode locking in fibre lasers affect the laser operation regime and the parameters of laser pulses. For example, laser pulses with durations in the range of 523–603 fs were achieved in [14] using different numbers of graphene layers. Sobon et al. [15] obtained pulses with durations from 501 to 530 fs using absorbers with different thicknesses based on carbon nanotubes.

To obtain passive mode locking in the present work, we used three samples of films with SWCNTs. We studied the influence exerted by the number of film layers and by the transmission coefficient of SWCNT films on the lasing characteristics of a dumbbell-shaped thulium fibre laser.

2. Fabrication and study of films with nanotubes

Single-walled carbon nanotubes with an average diameter of 2 nm (TuballTM) and a concentration of 0.1 mg mL^{-1} were mixed with 1% aqueous solution of carboxymethyl cellulose. Next, this suspension was exposed to 200-W ultrasound for 1.5 h to disintegrate SWCNT bunches and then centrifuged in a Beckman Coulter Optima MAX-E ultracentrifuge for 1 h with a rate of 50000 rpm. For further investigation, we separated supernatant (3 of 4 ml in the centrifuge tube) and diluted it with 1% aqueous solution of carboxymethyl cellulose by factors of 10, 5, and 3 (sample Nos 1, 2, and 3, respectively). After this, the suspensions were homogenised using a magnetic stirrer, poured into Petri dishes, and dried for three days to the complete evaporation of water. As a result, we obtained polymer films 15 μm thick containing SWCNTs. Taking into account the nanotube diameter, the absorption saturation relaxation time was estimated to be 1.8–2 ps [16].

The scheme of the setup for determining the optical transmission of absorbers is shown in Fig. 1. To determine the transmission coefficient in the saturated state, the radiation of a thulium laser (λ_0 = 1960 nm) with a pulse repetition rate of

A.D. Zverev Lomonosov Moscow State University, Vorob'evy Gory, 119991 Moscow, Russia; Prokhorov General Physics Institute, Russian Academy of Sciences, ul. Vavilova 38, 119991 Moscow, Russia; e-mail: izverevad@gmail.com;
V.A. Kamynin, A.I. Trikshev, N.R. Arutyunyan, E.D. Obraztsova, V.B. Tsvetkov Prokhorov General Physics Institute, Russian Academy of Sciences, ul. Vavilova 38, 119991 Moscow, Russia;
E.Yu. Kovtun Skolkovo Institute of Science and Technology, Bol'shoi bulv. 30, stroenie 1, 121205 Mocow, Russia;
A.A. Mastin, P.A. Ryabochkina Institute of Physics and Chemistry, N.P. Ogarev Mordovian State University, Bol'shevistskaya ul. 68A, korp. 2, 430005 Saransk, Russia

Received 19 March 2021
Kvantovaya Elektronika **51** (6) 518–524 (2021)
Translated by M.N. Basieva

5.3 MHz and a pulse duration of 2 ps was transmitted through the SWCNT samples. The average radiation power incident on the nanotubes was changed using a variable attenuator (VA) in the range from 0 to 2 mW (i.e., the pulse energy varied from 0 to 120 pJ). The transmission characteristics of the fabricated films were determined by comparing the pulse powers at outputs 1 and 2.

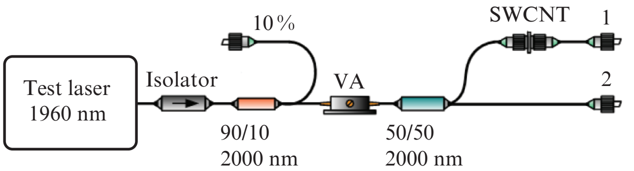

Figure 1. Scheme of the setup for determining the SWCNT transmission parameters: (VA) variable optical attenuator; (SWCNT) studied films with SWCNTs.

The dependences of the transmission of different absorbers on the pulse energy are presented in Fig. 2a. For precise determination of the initial (unsaturated) transmission of samples, the transmission of films in the unsaturated regime was measured on the setup shown in Fig. 1 using a cw thulium laser with the same wavelength (1960 nm) as a test source. The average power incident on the samples was changed from 1 to 5 mW. Since the measurements of absorption saturation in the pulsed regime showed that a noticeable saturation begins approximately from a peak power of 1 W, the use of cw lasers with such values of average power should not affect the transmission of samples. Comparing the radiation powers at outputs 1 and 2, we determined the transmission coefficients of the studied films depending on the incident cw power. The measured results are presented in Fig. 2b.

The measured transmission coefficients of the three studied samples of single-layer SWCNT films in the saturated (T_S) and non-saturated (T_{NS}) states are as follows: No. 1, T_S = 97% and T_{NS} = 76%; No. 2, T_S = 96% and T_{NS} = 65%; and No. 3, T_S = 87% and T_{NS} = 38%.

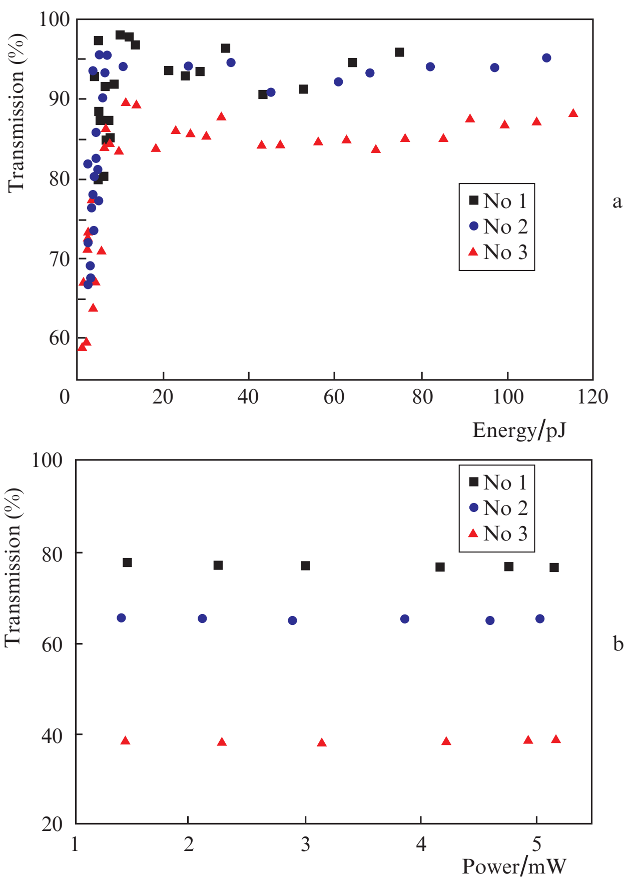

Figure 2. Dependences of the transmission of three SWCNT films on (a) propagating pulse energy and (b) cw radiation power.

3. Study of thulium fibre laser characteristics

The fabricated and characterised samples of absorbers were used to study the influence of the number of layers and the transmission coefficients of films with nanotubes on the operation regimes of a thulium fibre laser with a dumbbell-shaped cavity. The laser scheme is given in Fig. 3.

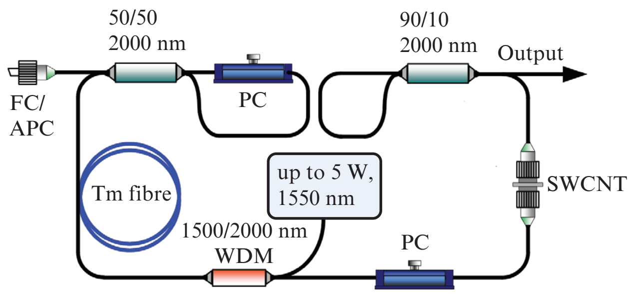

Figure 3. Scheme of a thulium laser with a dumbbell-shaped cavity: (PC) polarisation controller; (SWCNT) films with SWCNTs in a fibre-optic connector; (Tm fibre) active waveguide; (FC/APC) right-angle optical connector; (WDM) wavelength-division multiplexor.

A thulium-doped fibre (Eye Safe 9/125 Thulium-Doped Single-Mode Single Clad Fiber, Nufern) was pumped through a wavelength-division multiplexor WDM by a cw laser with a wavelength of 1550 nm and a power of up to 5 W. As cavity mirrors, we used two optical couplers with spliced ports on one side, namely, a 50/50 optical coupler as a highly reflecting mirror (the free coupler port terminated with a right-angle connector with a minimal backward reflection) and a 90/10 coupler as a partially transparent mirror. Passive mode locking was achieved by placing polymer films with SWCNTs between two FC/APC optical connectors. The lasing regime was adjusted by tuning polarisation controllers PCs. The laser characteristics were controlled from port 'Output'.

4. Experimental results

When using one layer of film No. 1 (T_S = 97%, T_{NS} = 76%), we failed to obtain stable pulsed laser regimes. Addition of the second layer (total transmission T_S = 94%, T_{NS} = 58%) allowed us to achieve a regular train of pulses (see the inset in Fig. 4a) with a period of 120 ns, which corresponds to the cavity roundtrip time. However, the output spectrum (Fig. 4a) exhibited a considerable continuous-wave fraction, which makes impossible to use this laser regime for subsequent amplification and practical application. A similar situation was observed for single-layer film No. 2 (T_S = 96%, T_{NS} = 65%). The spectral and temporal characteristics of the output radiation obtained with this film are presented in Fig. 4b.

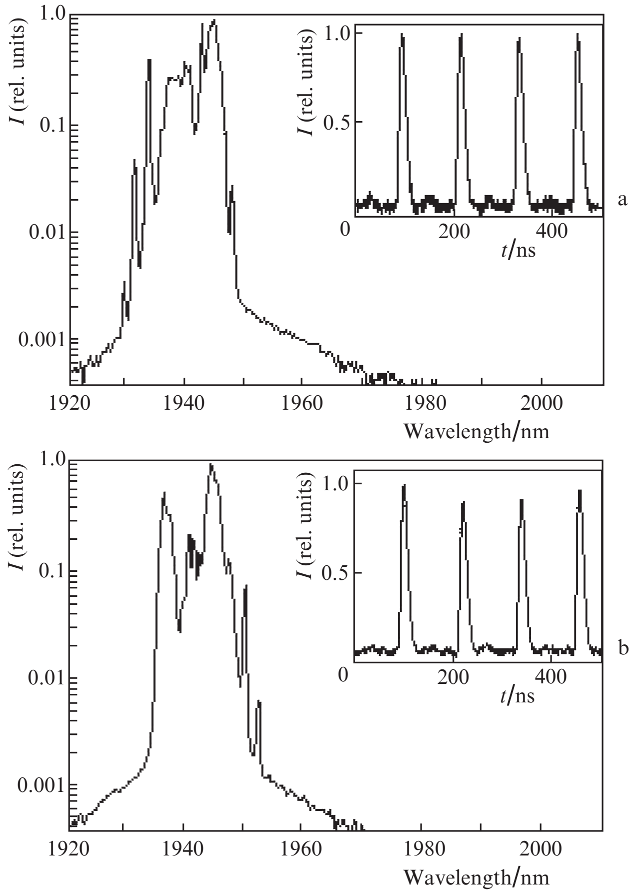

Figure 4. Emission spectra and (insets) pulse trains in the case of using (a) two layers of film No. 1 and (b) one layer of film No. 2.

The use of two-layer film absorber No. 2 (total transmission T_S = 92%, T_{NS} = 42%) allowed stable thulium laser operation in several regimes. At pump power P_p = 325 mW, the laser operated in a Q-switching (QS) regime. The average output power was 1.36 mW, the pulse repetition period was 110 μs, and the pulse duration was 6 μs. The oscillogram and the output spectrum in this regime are shown in Fig. 5. Note that the pump power was insufficient to excite a mode-locking (ML) regime due to the total losses in the cavity, including losses related to the presence of a saturable absorber, which did not prevent lasing in the pulsed QS regime.

The polarisation dependence of reflection of the loop mirrors of the thulium laser made it possible to decrease the total cavity losses using a polarisation controller, which allowed us, at the same pump power of 325 mW, to achieve a transient QS–ML regime, i.e., Q-switching with simultaneous mode locking. The repetition rate of pulses inside the QS pulse envelope was 8.4 MHz, and the average output power was 1.44 mW. The temporal and spectral characteristics of the output radiation in the QS–ML regime are presented in Fig. 6.

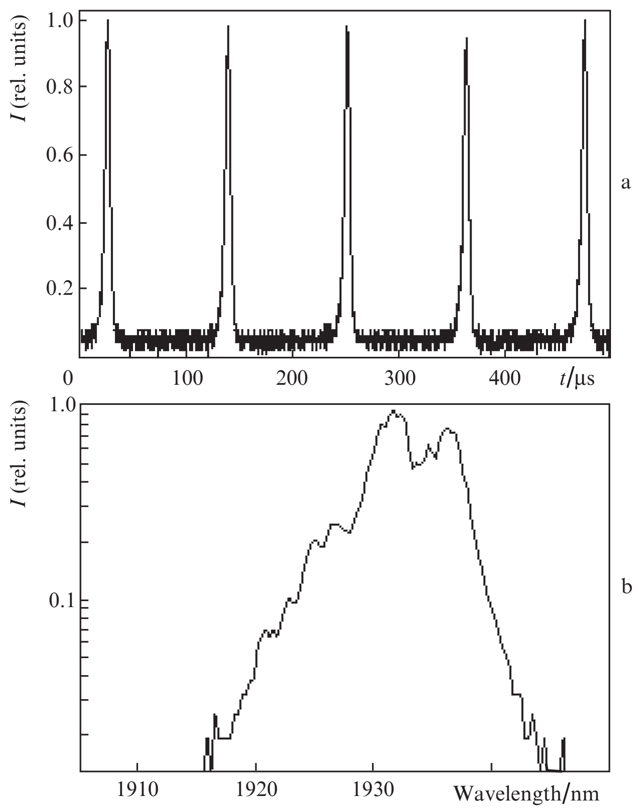

Figure 5. Oscillogram and (b) spectrum of laser radiation in the QS regime in the case of using two layers of film No. 2; P_p = 325 mW.

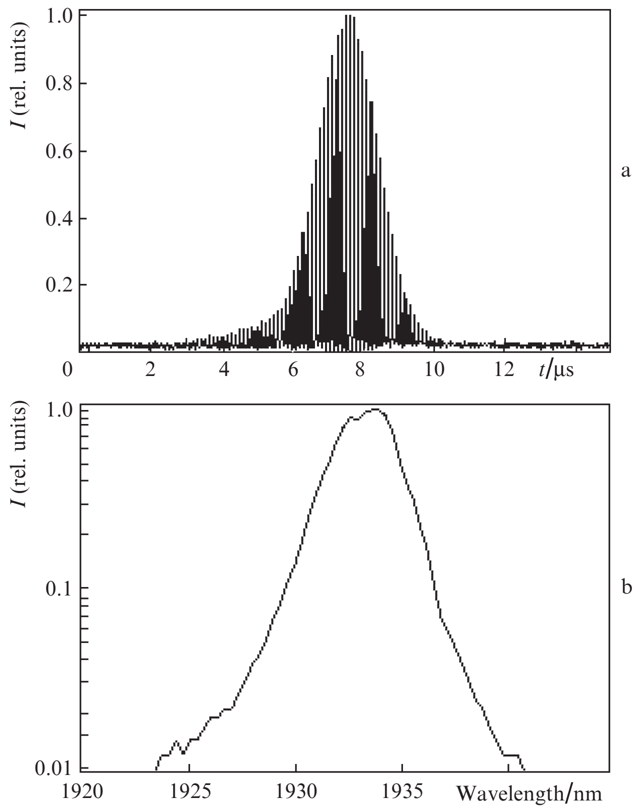

Figure 6. (a) Temporal and (b) spectral output characteristics of the thulium laser in the QS–ML regime in the case of two layers of film No. 2; P_p = 325 mW.

By additional adjustment of the polarisation controller, we obtained a pure mode-locking regime with a pulse repetition rate of 8.4 MHz at the same pump power (325 mW) (see the inset in Fig. 7a). The pulse duration τ_0 was estimated by the autocorrelation function (Fig. 7a) to be 1.08 ps, the average output power was 3.5 mW, and the laser band width at half maximum was 3.7 nm (Fig. 7b). The time-bandwidth product was 0.32, which is characteristic for unchirped solitons [17].

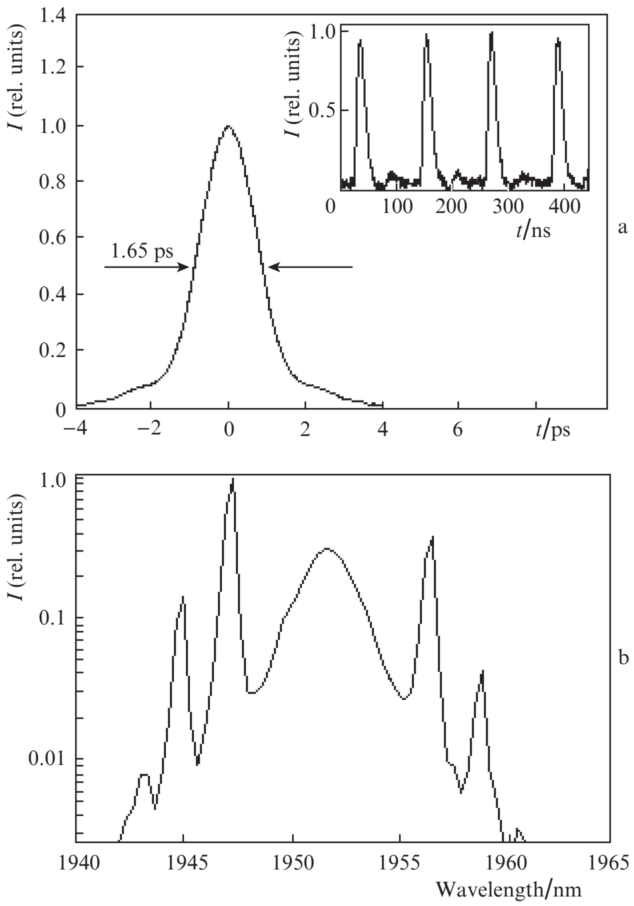

Figure 7. (a) Autocorrelation function and (inset) oscillogram of laser pulses, as well as (b) laser spectrum in the ML regime obtained by using two layers of film No. 2; P_p = 325 mW.

The laser spectrum (Fig. 7b) clearly shows Kelly peaks [18]. They appear as a result of soliton interference with a dispersive wave formed due to periodic variations in gain, losses, or dispersion upon pulse propagation in the cavity [19]. By the positions of these peaks, it is possible to determine the group velocity dispersion parameter (GVDP) from the formula [20]

$$\Delta_N = \frac{\ln(1+\sqrt{2})}{\pi}\sqrt{\frac{4N}{|\beta_{2\text{sum}}|L} - \frac{1}{\tau_0^2}}, \qquad (1)$$

where Δ_N is the difference between the frequency of the Nth Kelly peak and the centre frequency, τ_0 is the soliton duration, $\beta_{2\text{sum}}$ is the cavity GVDP, and L = 23.8 m is the cavity length. As a result, we obtain that the cavity GVDP at the centre wavelength λ_0 = 1951.1 nm is $\beta_{2\text{sum}} = -0.071$ ps^2 m^{-1}. Changing this parameter by adding fibre segments with different GVDPs, it is possible to achieve generation of conservative and dissipative solitons, as well as of stretched pulses [21].

The GVDPs of cavity components are related as

$$\beta_{2\text{SMF}}L_{\text{SMF}} + \beta_{2\text{Tm}}L_{\text{Tm}} = \beta_{2\text{sum}}L, \qquad (2)$$

where $\beta_{2\text{SMF}}$ is the GVDP of the single-mode fibre (SMF), L_{SMF} is the sum of the double length of the SMF in the linear cavity part and the length of the fibre used as mirrors, $\beta_{2\text{Tm}}$ is the GVDP of the thulium fibre, and L_{Tm} is the double thulium fibre length. Therefore, taking into account that L_{Tm} = 7 m, L_{SMF} = 17.2 m, and $\beta_{2\text{SMF}} = -0.068$ ps^2 m^{-1}, we find that the thulium fibre GVDP is $\beta_{2\text{Tm}} = -0.074$ ps^2 m^{-1}.

An increase in the pump power to 396 mW led to generation of dual pulses with an interval of 30 ns (Fig. 8a). This is caused by the fact that a soliton pulse propagating in a cavity with given dispersion and nonlinearity can have only a definite energy [9]. With increasing pump power and, hence, gain, which leads to an increase in the energy, pulses bifurcate. The pulse pair repetition period coincides with the cavity roundtrip time. The spectral characteristics of the output radiation in this regime are presented in Fig. 8b.

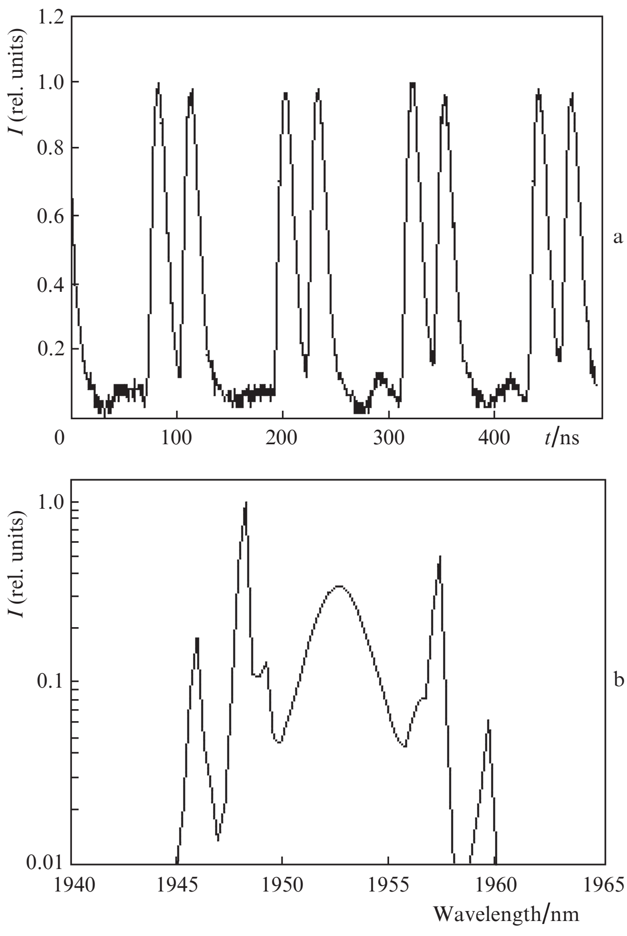

Figure 8. (a) Oscillogram and (b) spectral characteristics of laser radiation in the case of two layers of film No. 2; P_p = 396 mW.

In the case of using one layer of film No. 3 (T_S = 87%, T_{NS} = 38%), we also obtained stable lasing regimes, but at a higher pump power. At P_p = 396 mW, the laser operated in the QS regime with a pulse duration of 4 μs. As is seen from Fig. 9a, the pulse repetition period is 100 μs, and the average output power is 1.9 mW. The output laser spectrum is shown in Fig. 9b. Comparing this regime with the QS regime in the case of two layers of sample No. 2, we can conclude that the pulse repetition rate can be changed by changing the total losses in the cavity and the pump power.

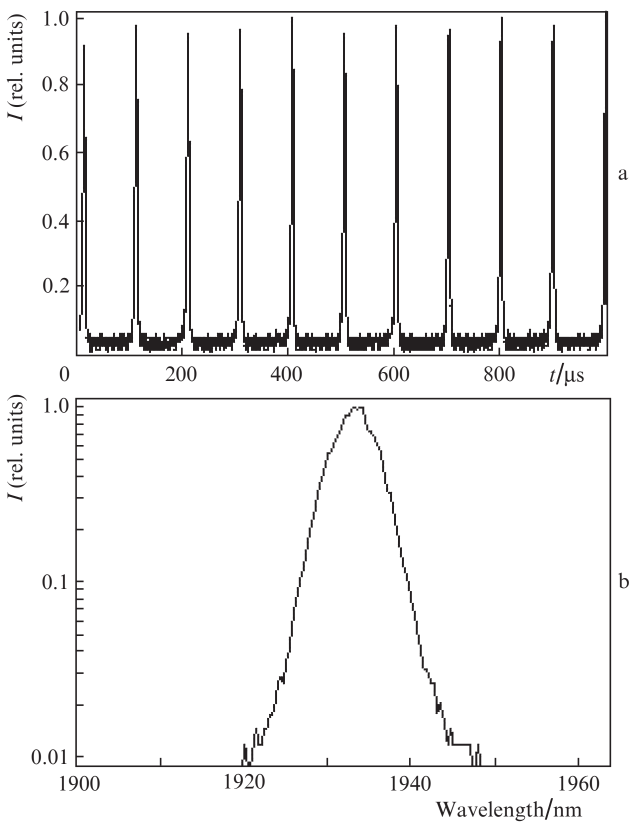

Figure 9. (a) Temporal and (b) spectral characteristics of output radiation in the QS regime in the case of one layer of film No. 3; P_p = 396 mW.

Using single-layer film No. 3, by changing polarisation controller position at a constant pump power, we obtained a QS–ML regime with an average output power of 2.1 mW. The pulse repetition rate inside the QS pulse envelope corresponded to the cavity roundtrip time. The oscillogram and spectrum of the output radiation are shown in Fig. 10.

At a pump power of 396 mW, we obtained the ML regime by adjusting the polarisation controller. The average output power was 3.2 mW (versus 3.5 mW obtained in the ML regime with the use of two layers of film No. 2), which testifies to a lower laser efficiency in this case. Figure 11a shows the autocorrelation function of the output radiation in the ML regime. The pulse duration was 1.05 ps, the spectral width at a level of –3 dB was 3.7 nm (Fig. 11b), and the period was 120 ns (see the inset in Fig. 11a). The corresponding time–bandwidth product was ~0.32, which, in combination with the presence of Kelly peaks in the laser spectrum, indicated the soliton regime of laser operation. By formulae (1) and (2), we also calculated the GVDPs of the cavity and thulium fibre at the

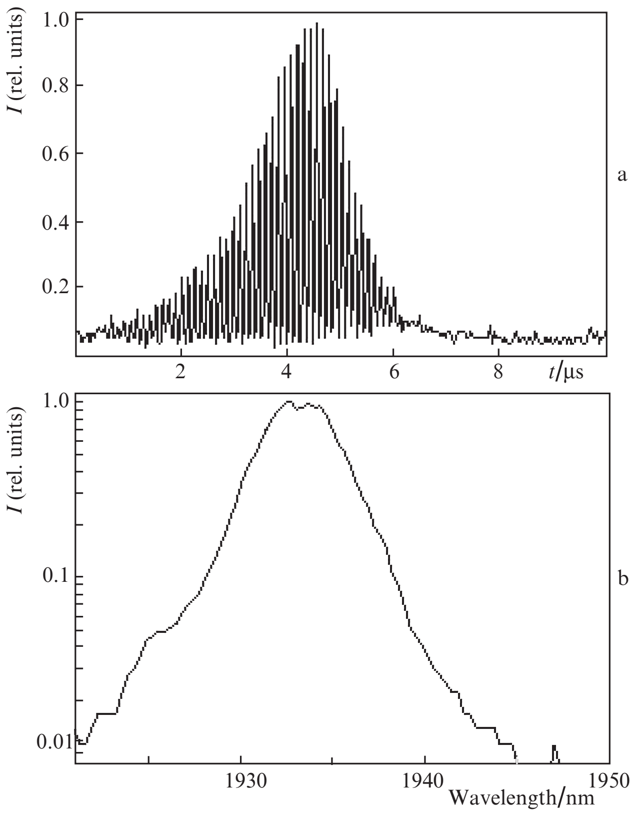

Figure 10. (a) Oscillogram and (b) spectrum of laser radiation in the QS–ML regime obtained using one layers of film No. 3; P_p = 396 mW.

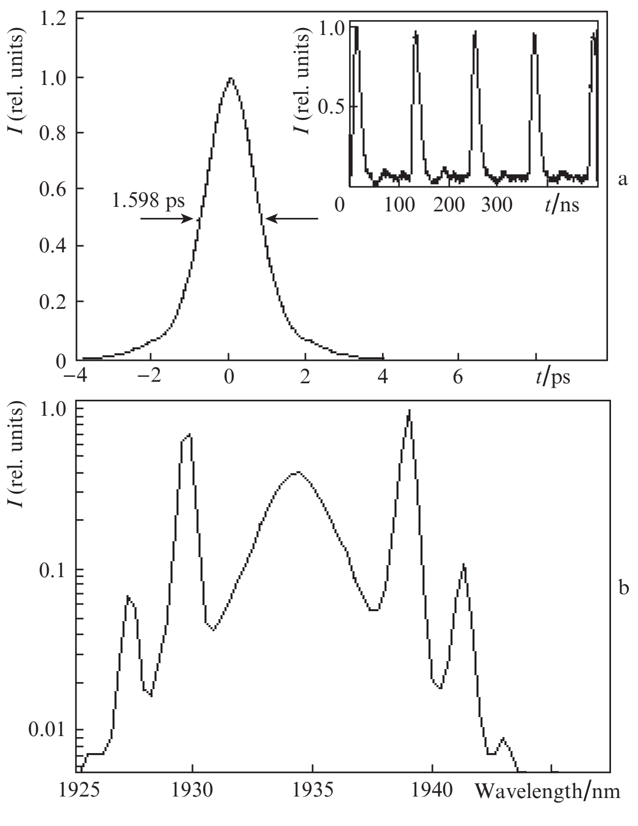

Figure 11. (a) Autocorrelation function and (inset) oscillogram of laser pulses, as well as (b) output radiation spectrum in the ML regime obtained using one layer of film No. 3; P_p = 396 mW.

centre wavelength λ_0 = 1934 nm to be $\beta_{2sum} = -0.069$ ps^2 m^{-1} and $\beta_{2Tm} = -0.067$ ps^2 m^{-1}, which is close to the above values.

Similar to the case with films No. 2, an increase in the pump power to 461 mW lead to soliton bifurcation and to the ML regime with dual pulses. The interpulse interval in this case was 40 ns (Fig. 12a). The laser spectrum in this operation regime is presented in Fig. 12b.

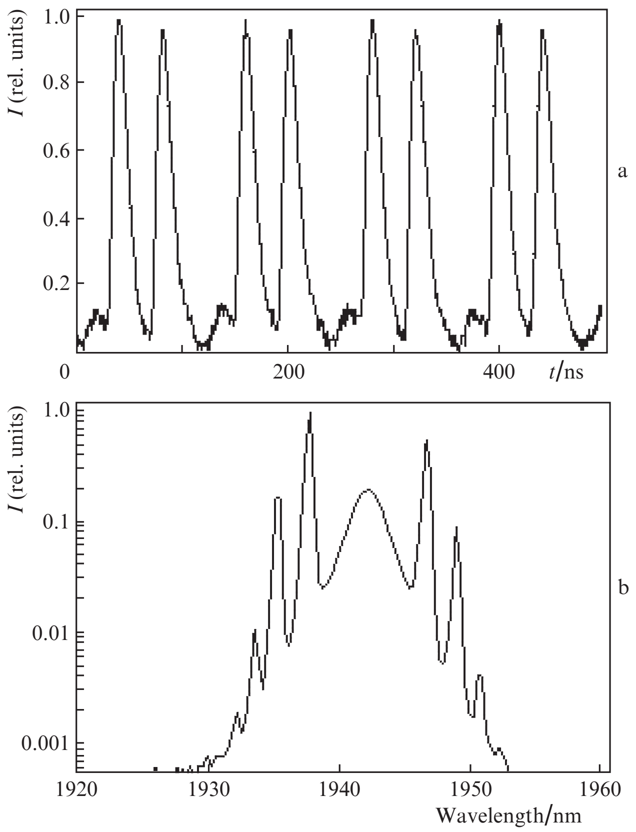

Figure 12. Figure 12. (a) Pulse train and (b) spectral characteristics of laser radiation in the case of one layer of film No. 3; P_p = 461 mW.

The experimental results are presented in Table 1, in which black cells correspond to unstable regimes, grey cells indicate the transient region, and uncoloured cells belong to stable regimes (ML–DP denotes the ML regime with dual pulses). For stable regimes, Table 1 also shows the pump power (in mW) at which lasing occurred. The pump power in the experiments varied from 100 to 500 mW, while higher pump powers caused breakdown of saturable absorbers.

Table 1. Experimental results.

Film samples	Transmission		Pump power/mW			
	T_S (%)	T_{NS} (%)	QS	QS–ML	ML	ML–DP
No. 1, one layer	97	76	100–500	100–500	100–500	100–500
No. 1, two layers	94	58	100–500	100–500	100–500	100–500
No. 2, one layer	96	65	100–500	100–500	100–500	100–500
No. 2, two layers	92	42	325	325	325	396
No. 3, one layer	87	38	396	396	396	461

Table 1 shows that we did not obtain stable pulsed laser regimes using polymer SWCNT films with non-saturated transmission $T_{NS} \geqslant 58\%$ (i.e., for single-layer film Nos 1 and 2 and two-layer film No. 1). This is related to the transition to a quasi-cw operation regime due to a high gain in the active fibre and a rather high Q-factor of the cavity at this T_{NS} level.

The use of two layers of SWCNT film No. 2 with a total transmission of 42% in the non-saturated state and 92% in the saturated state allowed us to achieve several stable operation regimes, namely, a QS regime with a pulse repetition period of 110 μs and a pulse duration of 6 μs, a QS–ML regime with an ML pulse repetition rate inverse to the cavity roundtrip time, an ML regime with a pulse repetition rate of 8.4 MHz and an average output power of 3.5 mW at a pulse duration of 1.08 ps, and an ML regime with dual pulses spaced by 30 ns.

When using one layer of SWCNT film No. 3 with T_{NS} = 38% and T_S = 87%, we obtained operation regimes similar to those observed with the use of two layers of film No. 2, but at a higher pump power. In the QS regime, the laser emitted pulses with a period of 100 μs and a duration of 4 μs, while the repetition period of ultrashort pulses in the QS–ML regime was 120 ns. In the ML regime with dual pulses, the interpulse interval was 40 ns. The output power in the single-pulse ML regime was 3.2 mW at a pulse repetition rate of 8.4 MHz and a pulse duration of about 1.05 ps. Thus, a decrease in transmission coefficients T_S and T_{NS} of SWCNT films led to a decrease in the laser efficiency.

Thus, we have demonstrated the influence of the saturable absorber parameters on the operation regimes of a dumbbell-shaped thulium fibre laser. The laser operation regimes are optimised for saturable absorber characteristics. It is shown that it is preferable to use two layers of SWCNT film No. 2 with total transmission coefficients of 92% in saturated and 42% in non-saturated states.

Acknowledgements. This work was performed at the World-Class Research Centre ‘Photonics’ and supported by the Ministry of Science and Higher Education of the Russian Federation (Project No. 075-15-2020-912).

References

1. Kerse C., Kalaycıoğlu H., Elahi P., Çetin B., Kesim D., Akçaalan Ö., Yavaş S., Aşık M.D., Öktem B., Hoogland H., Holzwarth R., Ilday F.Ö. *Nature*, **537** (7618), 84 (2016).
2. Potma E.O., Jones D.J., Cheng J.X., Xie X.S., Ye J. *Opt. Lett.*, **27** (13), 1168 (2002).
3. Sobon G., Klimczak M., Sotor J., Krzempek K., Pysz D., Stepien R., Martynkien T., Abramski K.M., Buczynski R. *Opt. Mater. Express,* **4** (1), 7 (2014).
4. Matsas V.J., Newson T.P., Richardson D.J., Payne D.N. *Electron. Lett.*, **28** (15), 1391 (1992).
5. Duling I.N. *Opt. Lett.*, **16** (8), 539 (1991).
6. Kivistö S., Okhotnikov O.G. *IEEE Photonics Technol. Lett.*, **23** (8), 477 (2011).
7. Filatova S.A., Kamynin V.A., Zhluktova I.V., Trikshev A.I., Arutyunyan N.R., Rybin M.G., Obraztsova E.D., Batov D.T., Voropaev V.S., Tsvetkov V.B. *Quantum Electron.*, **49** (12), 1108 (2019) [*Kvantovaya Elektron.*, **49** (12), 1108 (2019)].

8. Sotor J., Sobon G., Tarka J., Pasternak I., Krajewska A., Strupinski W., Abramski K.M. *Opt. Express*, **22** (5), 5536 (2014).
9. Yin K., Zhang B., Li L., Jiang T., Zhou X., Hou J. *Photonics Res*., **3** (3), 72 (2015).
10. Liu H., Zheng X., Liu M., Zhao N., Luo A., Luo Z., Xu W., Zhang H., Zhao C., Wen S. *Opt. Express*, **22** (6), 6868 (2014).
11. Chernysheva M.A., Krylov A.A., Arutyunyan N.R., Pozharov A.S., Obraztsova E.D., Dianov E.M. *IEEE J. Sel. Top. Quantum Electron*., **20** (5), 448 (2014).
12. Wang Q., Chen T., Chen K. *Proc. CLEO 2010* (OSA, 2010) p. CFK7.
13. Kieu K., Wise F.W. *IEEE Photonics Technol. Lett*., **21** (3), 128 (2009).
14. Liu C.N., Huang P.L., Cheng W.H., Yeh C.Y. *Proc. 2018 7th International Symposium on Next Generation Electronics* (ISNE) *2018* (Taiwan) pp 1 – 2.
15. Sobon G., Duzynska A., Świniarski M., Judek J., Sotor J., Zdrojek M. *Sci. Rep*., **7** (1), 1 (2017).
16. Ichida M., Hamanaka Y., Kataura H., Achiba Y., Nakamura A. *Phys. B: Condens. Matter*, **323** (1 – 4), 237 (2002).
17. Lazaridis P., Debarge G., Gallion P. *Opt. Lett*., **20** (10), 1160 (1995).
18. Kelly S.M.J. *Electron. Lett*., **28** (8), 806 (1992).
19. Ge Y., Guo Q., Shi J., Chen X., Bai Y., Luo J., Jin X., Ge Y., Li L., Tang D., Shen D., Zhao L. *Microw. Opt. Technol. Lett*., **58** (1), 242 (2016).
20. Lin Y.H., Lin G.R. *Laser Phys. Lett*., **10** (4), 045109 (2013).
21. Wang Y., Alam S.U., Obraztsova E.D., Pozharov A.S., Set S.Y., Yamashita S. *Opt. Lett*., **41** (16), 3864 (2016).